Pseudogap formation in four-layer $BaRuO_3$ and its electrodynamic response changes

Y. S. Lee, J. S. Lee, K. W. Kim, and T. W. Noh
School of Physics and Research Center for Oxide Electronics, Seoul National University, Seoul 151-747, Korea

Jaejun Yu
School of Physics and Center for Strongly Correlated Materials Research, Seoul National University, Seoul 151-747, Korea

Yunkyu Bang
Department of Physics, Chonnam National University, Kwangju 500-757, Korea

M. K. Lee and C. B. Eom
Department of Material Science and Engineering, University of Wisconsin-Madison, Madison, Wisconsin 53706
(Received 9 April 2001; revised manuscript received 28 June 2001; published 3 October 2001)

We investigated the optical properties of four-layer $BaRuO_3$, which shows a Fermi-liquid-like behavior at low temperature. Its optical conductivity spectra clearly displayed the formation of a pseudogap and the development of a coherent peak with decreasing temperature. Temperature dependences of the carrier density n and the scattering rate $1/\tau$ of the coherent component were also derived. As the temperature decreases, both n and $1/\tau$ decrease for four-layer $BaRuO_3$. These electrodynamic responses were compared with those of nine-layer $BaRuO_3$, which also shows a pseudogap formation but has an insulatorlike state at low temperature. It was found that the relative rates of change of both n and $1/\tau$ determine either metallic or insulatorlike responses in the ruthenates. The optical properties of the four-layer ruthenate were also compared with those of other pseudogap systems, such as high-T_c cuprates and heavy-electron systems.

DOI: 10.1103/PhysRevB.64.165109 PACS number(s): 78.30.−j, 78.66.−w

I. INTRODUCTION

Recently, ruthenates have attracted a great deal of attention due to their physical properties, exhibiting many unusual characteristics of strongly correlated electron systems, such as unconventional superconductivity in layered perovskite Sr_2RuO_4 (Ref. 1) and bad metallic non-Fermi-liquid behaviors in perovskite $SrRuO_3$.[2] Although the ruthenate systems belong to 4*d* transition metal oxides, electron-electron interactions are expected to be important in determining their physical properties. More recently, we reported a pseudogap formation in the nine-layer rhombohedral ($9R$) $BaRuO_3$, which can be considered as another kind of pseudogap system.[3]

Pseudogap phenomena have been intensively investigated in some strongly correlated electron systems. In high-T_c superconductors (HTSC), which are 3*d* transition metal oxides, pseudogap features with a reduction in the density of state at the Fermi energy $N(E_F)$ were observed especially in the underdoped regime. These features have attracted lots of interests due to their possible connection to the mechanism for the high-T_c superconductivity.[4–6] In some *f*-electron systems, such as UPt_3 (Ref. 7) and UPd_2Al_3,[8] pseudogaps were observed as well as heavy fermion (HF) behaviors, which are due to the large enhancement of the effective mass m^* of quasiparticles.[9] In both systems, the scattering rate $1/\tau$ of quasiparticles was found to be suppressed with pseudogap formation. Although many investigations have been performed, the basic mechanisms of pseudogap formation have not yet been fully understood.

Our early observation of a pseudogap in $9R$ $BaRuO_3$ suggests that the ruthenate could be another material with fascinating electronic properties.[3] Compared to the cases of HTSC and HF systems, our optical spectra show clearer electrodynamic response changes with pseudogap formation. It was found that $9R$ $BaRuO_3$ can have a metallic state in spite of a large reduction of carrier density n after the pseudogap was formed. This unusual behavior is found to be closely related to a very significant reduction in $1/\tau$. It was also suggested that the pseudogap formation could be related to structural characteristics of the layered compound, which is shown in Fig. 1(a).[10] In the $9R$ structure, three adjacent RuO_6 octahedra have face sharings, which result in quasi-one-dimensional (1D) metal-bondings along the *c* axis. Then, a 1D-like instability fluctuation, such as a charge density wave (CDW) instability, could contribute to the pseudogap formation.

To obtain further understanding, it would be useful to investigate electrodynamic responses of ruthenates with simi-

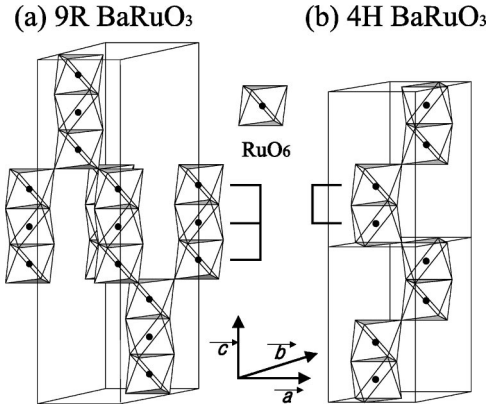

FIG. 1. Schematic diagrams of two crystallographic forms of $BaRuO_3$: (a) $9R$ phase, (b) $4H$ phase.

lar crystal structures. Bulk $BaRuO_3$ is known to have three crystal structures:[10–12] (i) the $9R$, (ii) the six-layered hexagonal ($6H$), and (iii) the four-layered hexagonal ($4H$) structures. The $9R$ $BaRuO_3$ phase has been considered the most stable bulk form. On the other hand, $6H$ and $4H$ $BaRuO_3$ are known to be difficult to synthesize reproducibly under ordinary conditions. Recently, some of us (M.K.L. and C.B.E.) successfully synthesized epitaxial $4H$ BaRuO3 films.[13,14] As shown in Fig. 1(b), $4H$ $BaRuO_3$ has two adjacent RuO_6 octahedra with a face sharing, so the quasi-1D metal bonding can also occur along the c axis. However, the 1D-like contribution in the $4H$ compound will be weaker than that in $9R$ $BaRuO_3$.

In spite of the structural similarities, some physical properties of these layered compounds are quite different.[15] While the dc resistivity $\rho(T)$ curve of $9R$ $BaRuO_3$ shows a crossover behavior from a metallic to an insulatorlike state at a low temperature (T), $4H$ $BaRuO_3$ remains in a metallic state down to very low T. It is known that $BaRuO_3$ systems are nonmagnetic and are expected to have Pauli paramagnetism. As T decreases, the magnetic susceptibility $\chi(T)$ of $4H$ $BaRuO_3$ increases slightly, however, that of $9R$ $BaRuO_3$ decreases.[15] These differences in the physical properties can originate from subtle differences in the T dependence of electrodynamic quantities, such as n, $1/\tau$, and m^*. However, there are no systematic studies on these intriguing quantities of $4H$ $BaRuO_3$.

In this paper, we report the optical properties of $4H$ $BaRuO_3$. Its optical conductivity spectra $\sigma_1(\omega)$ show pseudogap formation and the development of a coherent component in the far-infrared region. With the pseudogap formation, n decreases and $1/\tau$ becomes suppressed. The stronger T dependence of $1/\tau$ will make this material metallic down to very low T. From these observations, we suggest that the 1D-like instability fluctuation could also be involved in $4H$ $BaRuO_3$, but weaker than that in $9R$ $BaRuO_3$. The T dependences of the electrodynamic quantities will also be discussed in order to explain the differences in $\rho(T)$ and $\chi(T)$ in the layered $BaRuO_3$ compounds.

II. EXPERIMENTAL RESULTS

A. Sample preparation and characterization

A high quality $4H$ $BaRuO_3$ epitaxial film was fabricated on a $SrTiO_3(111)$ substrate using a 90° off-axis sputtering technique.[13] X-ray diffraction and transmission electron microscopy studies revealed that the film is composed of single domains of c-axis $4H$ structures with an in-plane epitaxial arrangement of $BaRuO_3[2110]\|SrTiO_3[110]$. Most measurements reported in this paper were performed to probe properties parallel to the film, namely ab-plane responses of $4H$ $BaRuO_3$.

The $\rho(T)$ curve was measured using the standard four probe method. As shown in Fig. 2, $4H$ $BaRuO_3$ has a metallic state down to 4 K. Above 220 K, $\rho(T)$ seems to have a linear T dependence, which has been often observed in other bad metallic materials, such as $SrRuO_3$. In $4H$ $BaRuO_3$, the room temperature resistivity is comparable to the Mott critical resistivity $\rho_{\mathrm{Mott}}=3\hbar a/e^2\simeq 660\ \Omega$ cm, where a is a lattice constant of the ab plane. So, the linear T dependence of $\rho(T)$ near the room temperature region might be related to the behavior of a bad metal. On the other hand, as shown in the inset of Fig. 2, the T dependence of $\rho(T)$ at low T can scale with T^2, indicating that $4H$ $BaRuO_3$ has a Fermi liquidlike behavior. This strong Fermi liquid behavior can be evidently distinguished from the insulatorlike behavior of $9R$ $BaRuO_3$ below 110 K.

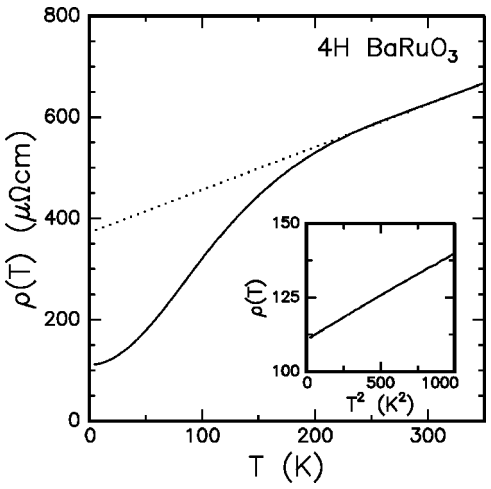

FIG. 2. T-dependent $\rho(T)$ curve. The inset shows the linear T^2 dependence of $\rho(T)$ curve at low T. The dotted line represents a linear T dependence at high T.

B. Reflectivity measurements

Near-normal incident reflectivity spectra, $R(\omega)$, of the ab-plane were measured in a wide photon energy region of 5 meV $\sim$30 eV with T variations. We used a conventional Fourier transform spectrophotometer between 5 meV and 0.6 eV. Between 0.5 eV and 6.0 eV, we used grating spectrometers. Above 6.0 eV, we used the synchrotron radiation from the normal incidence monochromator beam line at Pohang Accelerator Laboratory. To eliminate measurement errors due to the reflected light from the film/substrate interface, we used a very thick film whose thickness was about 1.1 μm. Then, the penetration depth, $\delta\sim c/\sqrt{2\pi\omega\sigma}$, of a light at 100 cm^{-1} was estimated to be about 0.6 μm at 300 K. Since the film thickness is larger than δ, the contribution of the reflected light from the film/substrate interface could be negligible. So, the strong phonon absorption peaks due to the $SrTiO_3$ substrate could not be observed in $R(\omega)$.

Figure 3 shows T-dependent $R(\omega)$ of $4H$ $BaRuO_3$ in the far-infrared (IR) region. The inset of Fig. 3 shows $R(\omega)$ of $4H$ $BaRuO_3$ in a wider frequency region. The level of $R(\omega)$ at 300 K is high in the far-IR region in agreement with the fact that it is in a metallic state. In addition, $R(\omega)$ below 200 cm^{-1} are highly consistent with predictions of the Hagen-Rubens relation, $R\simeq 1-(2\omega\rho/\pi)^{1/2}$.[16] However, $R(\omega)$ show an interesting crossover behavior: as T decreases, the reflectivity becomes strongly suppressed in the region between 200 cm^{-1} and 500 cm^{-1}. This crossover be-

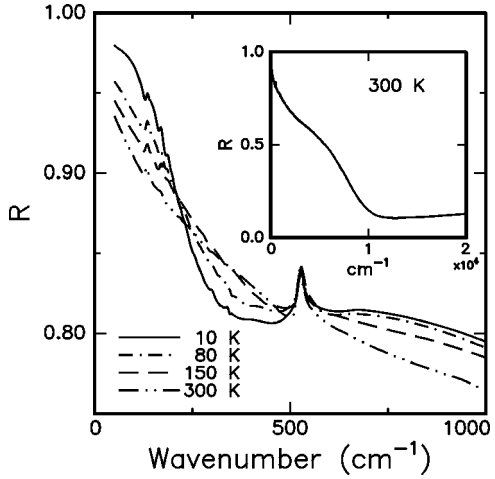

FIG. 3. T-dependent $R(\omega)$ below 1000 cm^{-1}. In the inset, $R(\omega)$ at 300 K in a wide frequency range is shown.

havior is different from a typical metallic response, indicating that $4H$ $BaRuO_3$ could have an unusual metallic state.

III. DATA ANALYSIS AND RESULTS

A. Optical conductivity spectra

The Kramers-Kronig (KK) transformation was used to calculate complex optical conductivity spectra, $\tilde{\sigma}(\omega) \equiv \sigma_1(\omega) - i(\omega/4\pi)\varepsilon_1(\omega)$, from the experimental $R(\omega)$. Here, $\varepsilon_1(\omega)$ represent real dielectric function spectra. For the KK transformation, $R(\omega)$ in the low frequency region were extrapolated with the Hagen-Rubens relation.[16] The calculated $\sigma_1(\omega)$ were found to be consistent with the experimental $\sigma_1(\omega)$ independently obtained by spectroscopic ellipsometry techniques in the visible region. These consistencies demonstrate the validity of our KK analysis.[17] The details of this analysis are published elsewhere.[18]

Figure 4 shows T-dependent $\sigma_1(\omega)$ obtained through the KK analysis in a wide frequency region. The strong peak at 550 cm^{-1} and several weak peaks below 500 cm^{-1} are due to transverse optic phonon modes. At 300 K, $\sigma_1(\omega)$ seems to

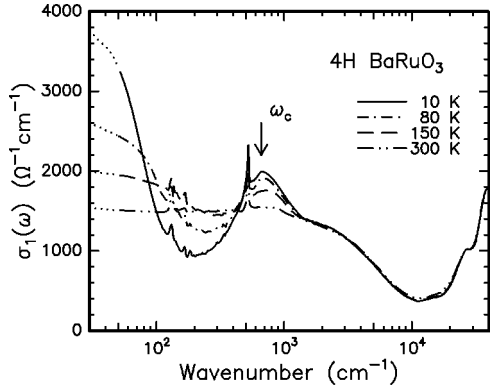

FIG. 4. T-dependent $\sigma_1(\omega)$ of $4H$ $BaRuO_3$ with a logarithmical scale of the bottom axis. The dotted lines are $\sigma_1(\omega)$ obtained from the Hagen-Rubens extrapolations. The arrow represents ω_c, the pseudogap position.

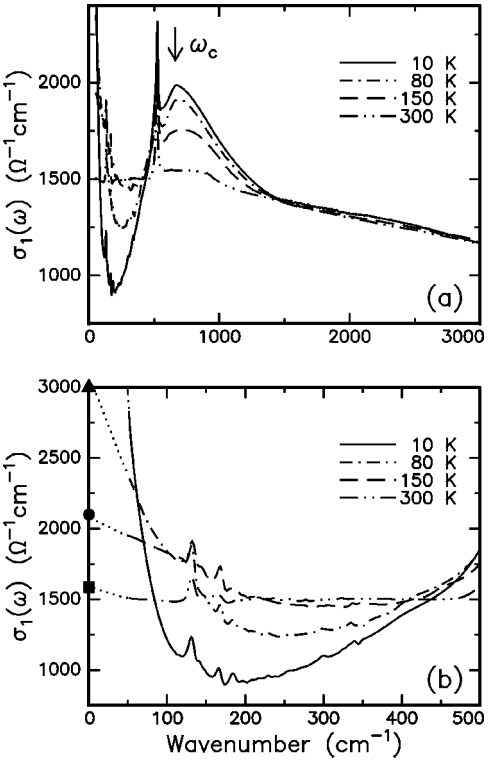

FIG. 5. (a) T-dependent $\sigma_1(\omega)$ below 3000 cm^{-1}. ω_c represents the pseudogap value. (b) $\sigma_1(\omega)$ below 500 cm^{-1} shown in detail. The solid triangle, solid circle, and solid square represent the dc $\sigma(T)$ at 80, 150, and 300 K, respectively. The dotted lines are $\sigma_1(\omega)$ obtained from Hagen-Rubens extrapolation.

show a Drude-like behavior with a very large value of $1/\tau$. As T decreases, however, the spectral weight below 500 cm^{-1} becomes suppressed and the spectral weight near 800 cm^{-1} increases, forming a gaplike feature. This feature is different from the formation of a normal energy gap in an insulator (or a semiconductor), where the spectral weight in the gaplike region should vanish completely. The remainder of the spectral weights in the gaplike region indicates that a pseudogap is formed in this material.

Figure 5(a) shows the pseudogap formation of $4H$ $BaRuO_3$ in more detail. One of the most important experimental facts is that the sum rule is satisfied: when $\sigma_1(\omega)$ is integrated up to 1.0 eV, the optical strength remains nearly constant. This means that most of the missing spectral weights in the gaplike region are transferred to higher frequencies, especially near 650 cm$^{-1} \simeq 0.08$ eV. [From now on, let us call the peak frequency position of $\sigma_1(\omega)$ the pseudogap position, ω_c.] Another interesting fact is that most of the spectral weight gain occurs near ω_c. Above 1400 cm^{-1}, the T dependence of the spectral weight changes is quite small. The significant spectral weight gain just above ω_c is also different from that of the normal energy gap formation, where the missed spectral weight is redistributed in much wider frequency regions.

Note that the pseudogap is formed in the metallic region, judged from $\rho(T)$. This fact is also related to a clear development of a strong Drude-like component in the far-IR region, as shown in Fig. 5(b). As T decreases, $\sigma_1(\omega)$ show that

a coherent Drude-like component becomes more evident: the value of $\sigma_1(\omega)$ in the low frequency region becomes larger and the width of the coherent component becomes smaller. The concurrent development of the pseudogap and coherent peak was also observed in $9R$ $BaRuO_3$,[3] however, such phenomena are more clearly seen in the $4H$ compound.

B. Inapplicability of the single component analyses

The optical responses of free carriers are usually analyzed in terms of the simple Drude model:

$$\tilde{\sigma}(\omega) \equiv \sigma_1(\omega) - i\frac{\omega}{4\pi}\varepsilon_1(\omega) = \frac{\omega_p^2}{4\pi}\frac{\tau}{(1-i\tau\omega)}, \qquad (1)$$

where the plasma frequency, $\omega_p = \sqrt{4\pi n e^2/m^*}$, represents the spectral weight of free carriers. However, we cannot apply this formula to explain the measured $\tilde{\sigma}(\omega)$ up to 1.0 eV. The room temperature data, shown in Fig. 4, might be approximately explained in terms of this formula. Then, the value of $1/\tau$ could be estimated to be about 4500 cm^{-1}. This value is so large that it seems difficult to explain the metallic state of this material. On the other hand, as shown in Fig. 5(b), the apparent $1/\tau$ at 10 K for the coherent component falls below 100 cm^{-1}, much lower than the estimated value at room temperature. This suggests that all of the T-dependent $\tilde{\sigma}(\omega)$ up to 1.0 eV cannot be explained in terms of the simple Drude model.

In many strongly correlated systems, optical responses of quasiparticles have been explained in terms of the frequency-dependent scattering rate $1/\tau(\omega)$ and effective mass enhancement $m^*(\omega)$.[19] Under such assumptions, the optical responses can be described in terms of the extended Drude model:

$$\tilde{\sigma}(\omega) = \frac{\omega_p^2}{4\pi}\frac{\tau(\omega)}{[1-i\omega m^*(\omega)\tau(\omega)]}. \qquad (2)$$

By using Eq. (2), both $m^*(\omega)$ and $1/\tau(\omega)$ can be derived directly from the experimental $\tilde{\sigma}(\omega)$. For most pseudogap materials, such as HTSC and HF systems, their optical responses have been interpreted in terms of this model.[9,20] However, we found that it was difficult to extend such single component analysis to the $4H$ $BaRuO_3$ case. Figures 6(a) and 6(b) show $1/\tau(\omega)$ and $m^*(\omega)$ obtained from an analysis based on the extended Drude model, respectively. Near ω_c, both $1/\tau(\omega)$ and $m^*(\omega)$ do not make sense. Especially, $m^*(\omega)$ becomes negative in the frequency region near ω_c, which is inadequate from a physics point of view. Therefore, the single component analysis based on the extended Drude model cannot also be applied to this layered ruthenate system.

C. T dependence of electrodynamic quantities using the two component analysis

For quantitative analysis of the T-dependent coherent component, we fitted the complex optical conductivity $\tilde{\sigma}(\omega)$ up to 1.0 eV using a two-component model. At each temperature, the coherent component in the far-IR region and gaplike feature near ω_c were fitted with the simple Drude model in Eq. (1) and the Lorentz oscillator model, respectively. The fitting results for $1/\tau$ and ω_p^2 of the coherent components are shown in Fig. 7.

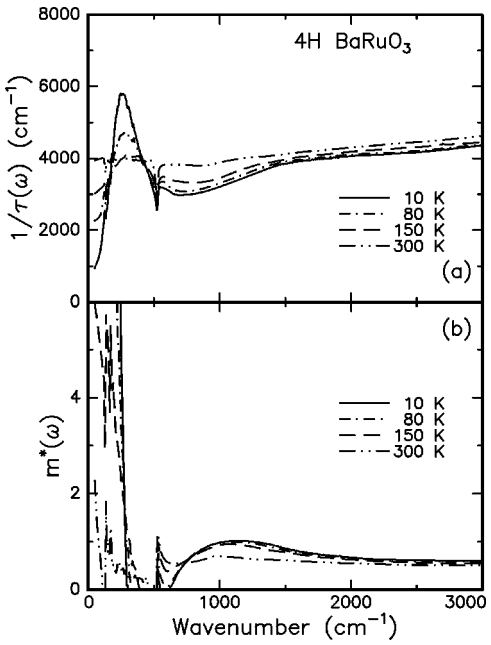

FIG. 6. T-dependent (a) $1/\tau(\omega)$ and (b) $m^*(\omega)$ derived from the extended Drude model analysis with $\omega_p \simeq 2.3$ eV.

It is noted that ω_p^2, which is proportional to the spectral weight of the coherent component, is reduced as the pseudogap develops. In general, the reduction of ω_p^2 can occur either by a reduction of n or by an enhancement of m^*. For approximate estimation of n and m^*, we used the three-dimensional free electron gas model. In this model, $\chi \propto m^* n^{1/3}$ and $\omega_p^2 \propto n/m^*$. With the previous reported values of $\chi(T)$,[15] the free electron gas model provides $n \simeq 8.3 \times 10^{21}$ cm^{-3} and $m^*/m_e \simeq 36$ at 10 K for $4H$ $BaRuO_3$, so its mean free path l can be estimated to be about 19 Å. At 300 K, the model provides $n \simeq 1.2 \times 10^{22}$ cm^{-3} and $m^*/m_e \simeq 27$, where m_e is a bare electron mass, so l will be about 4 Å.[21] This value is comparable to the lattice constant of the

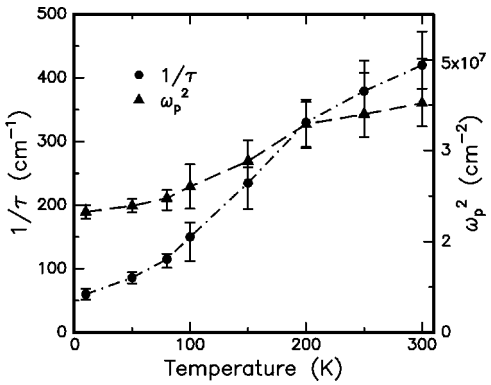

FIG. 7. T-dependent ω_p^2 and $1/\tau$ of the coherent component in $4H$ $BaRuO_3$.

ab plane, i.e., about 5.7 Å, which could be related to its bad metallic behavior, mentioned in Sec. II A.

In spite of the reduction of n, $4H$ $BaRuO_3$ has a metallic state down to low T. This unusual behavior can be explained by T-dependent changes in ω_p^2 and $1/\tau$. As shown in Fig. 7, $1/\tau$ might decrease significantly. According to the Drude model, dc electric resistivity $\rho_{\rm dc}$ is inversely proportional to ω_p^2 and τ. So, the relative changes in ω_p^2 and $1/\tau$ are important for determining a metallic or an insulatorlike behavior in ρ_{dc}. If the decrease in $1/\tau$ is larger than the reduction of n, a metallic state can be induced. The strong T-dependent rapid decrease in $1/\tau$ can explain the metallic behavior of $4H$ $BaRuO_3$, which might be closely related to the origin of the pseudogap.

IV. DISCUSSION

A. Fermi liquid behaviors of $4H$ $BaRuO_3$

Contrary to the $9R$ compound, $4H$ $BaRuO_3$ shows a Fermi liquid behavior in a low-T region. As shown in the inset of Fig. 2, its T dependence of $\rho(T)$ at low T can scale as T^2, indicating that $4H$ $BaRuO_3$ has Fermi liquid behavior. The fact that the T^2 scaling is valid in a relatively large-T region suggests that the electron-electron interaction is quite strong in this layered ruthenate.[22] From the relation $\rho(T) = \rho_o + AT^2$, A is found to be about $2.9\times10^{-2}\mu\Omega$ cm/K^2. This value is comparable with that found by a previous report on the $4H$ $BaRuO_3$ single crystal.[15]

We can estimate a linear coefficient in the specific heat γ to be about 55 mJ/mol K^2, using the universal relation, $A/\gamma^2 \simeq 1.0\times10^{-5}\mu\Omega$ cm (mol K/mJ)^2.[23] A similar value of γ can be obtained from a reported value of $\chi(T)\simeq 7\times10^{-4}$ emu/cm^3 within the standard free-electron model.[15] It is interesting to note that these values are comparable with those of Sr_2RuO_4 with a superconducting ground state ($\chi \simeq 9.7\times10^{-4}$ emu/mol and $\gamma\simeq 39$ mJ/mol K^2 for K).[1] Compared with the corresponding values for a typical Pauli paramagnetic metal (e.g., $\gamma\simeq 0.7$ mJ/mol K^2 for Au; $\chi\simeq 2.6\times10^{-5}$ emu/mol for K),[24] the values of γ and χ might be greatly enhanced. For Sr_2RuO_4, the value of $\chi(T)$ is significantly about 15 times that expected from the standard free electron model with $n\simeq 2.0\times10^{22}$ cm^{-3} and $m^*\simeq 2m_e$. This enhancement has been explained by ferromagnetic fluctuations.[25] Judging from the case of Sr_2RuO_4, it is possible that the ferromagnetic fluctuation might also be related to the large value of $\chi(T)$ in $4H$ $BaRuO_3$.[26] To clarify this possibility, further investigations are necessary.

B. Comparisons between $4H$ and $9R$ $BaRuO_3$

The optical spectra of $4H$ and $9R$ $BaRuO_3$ show the pseudogap formation and the development of the coherent components. As T decreases, both of the ruthenates show a reduction in ω_p^2 and suppression in $1/\tau$. (Refer to Fig. 7 of this paper and Fig. 3 of Ref. 3.) Although the general trends in the T dependences of the electrodynamic quantities are similar, some of their transport and magnetic properties are different.[15] These differences should be explained in terms of subtle differences of the T dependences in the electrodynamic quantities.

While $4H$ $BaRuO_3$ remains in a metallic state down to a very low T, the $\rho(T)$ curve of $9R$ $BaRuO_3$ shows a crossover behavior from a metallic (i.e., $d\rho/dT>0$) to an insulatorlike state (i.e., $d\rho/dT<0$) around 110 K.[3] Since $\rho_{\rm dc}$ is inversely proportional to ω_p^2 and τ, the relative changes in ω_p^2 and $1/\tau$ will determine a metallic or an insulatorlike state in $\rho(T)$. For $4H$ $BaRuO_3$, the decrease in $1/\tau$ is larger than that for ω_p^2 at all temperatures, as shown in Fig. 7. So, $d\rho/dT>0$ for all temperatures. On the other hand, for $9R$ $BaRuO_3$, the reduction in $1/\tau$ dominates and leads to metallic behavior above 110 K. However, at low T, the reduction in ω_p^2 is quite considerable and the inelastic relaxation time can become very large, so the disorder-induced scattering starts to play an important role. Then, the decrease in $1/\tau$ becomes smaller than that for ω_p^2, resulting in the insulatorlike state of $d\rho/dT<0$.

As T decreases, the magnetic susceptibility $\chi(T)$ of $4H$ $BaRuO_3$ increases slightly, however, that of $9R$ $BaRuO_3$ decreases.[15] It is known that both of the $BaRuO_3$ systems are nonmagnetic and are expected to have Pauli paramagnetism, whose contribution is proportional to $m^*n^{1/3}$. Note that $\omega_p^2 \propto n/m$, and that the changes in ω_p^2 of the $4H$ and $9R$ $BaRuO_3$ are about a factor of 2 and 30, respectively. The larger change in ω_p^2 of $9R$ $BaRuO_3$, which is due to a significant reduction in n, results in a decrease in $\chi(T)$. On the other hand, for $4H$ $BaRuO_3$, the subtle competition between weakly T-dependent $n(T)$ and $m^*(T)$ can enhance $\chi(T)$ slightly.

C. Comparisons with other pseudogap systems

In the case of underdoped HTSC, $\sigma_1(\omega)$ in the ab plane shows only weak spectral weight changes, so it is not easy to address the pseudogap formation based solely on $\sigma_1(\omega)$. However, when the extended Drude model is used, $1/\tau(\omega)$ shows a strong suppression in the low frequency region, which has been identified as a signature of the pseudogap.[27] On the contrary, $\sigma_1(\omega)$ along the c axis exhibits a suppression of the spectral weight in the far-IR region, which can be easily interpreted as a feature of the pseudogap.[28] However, it has been observed in the insulating state. On the other hand, $BaRuO_3$ systems show the clear pseudogap formation in $\sigma_1(\omega)$ of the metallic state. The features due to the pseudogap are so distinct that the extended Drude model analysis cannot be applied in the frequency region near ω_c, which is addressed in Sec. II B.

Pseudogap formations in $\sigma_1(\omega)$ have been also observed in some HF systems, such as UPt_3 (Ref. 7) and UPd_2Al_3.[8] However, the very small pseudogap size ($\sim$0.01 eV) and the extremely small spectral weight of the coherent mode hindered detailed analysis in connection with development of the pseudogap. For HF systems, the electrodynamic quantities were analyzed by the extended Drude model, assuming no change in n with the pseudogap formation. With decreasing T, $1/\tau(\omega)$ is also suppressed and $m^*(\omega)$ becomes en-

TABLE I. Summary of the changes of electrodynamic quantities with pseudogap formation in the various pseudogap systems.

	HTSC[a]	HF systems[b]	$BaRuO_3$
Anisotropy	strong	weak	weak
n	constant	constant	decrease
$1/\tau$	suppressed	strongly suppressed	strongly suppressed
m^*	nearly constant	largely enhanced	nearly constant
Pseudogap origin		hybridization	1D CDW fluctuation
Pseudogap size (eV)	~ 0.1	~ 0.01	~ 0.1
Pseudgap feature in $\sigma_1(\omega)$	weak	strong	strong

[a]Reference 29.
[b]References 9 and 30.

hanced significantly. The enhancement of $m^*(\omega)$ in the far-IR region has been explained by a strong renormalization of quasiparticles due to interactions with localized f electrons,[9] which could be the origin of HF behavior. On the other hand, our $BaRuO_3$ is a nonmagnetic material with no f electrons. In contrast to the case of HF systems, a reduction in n is clearly observed with the pseudogap formation, and the single component analysis based on the extended Drude model is not adequate to describe the spectral weight changes. As shown in Sec. III C, the two component model can describe its spectral weight changes better. The comparison in the electrodynamic quantities between $BaRuO_3$ and other pseudogap materials is summarized in Table I.

D. The origin of the pseudogaps in $BaRuO_3$: CDW fluctuations

In our earlier paper on $9R$ $BaRuO_3$, we argued that the origin of the pseudogap in the ruthenate should be the CDW fluctuations. Due to the quasi-1D metal-metal bondings along the c axis, shown in Fig. 1, such 1D instability fluctuations can make a contribution. There are a few other experimental facts which support this suggestion. First, $BaIrO_3$, isostructural with $9R$ $BaRuO_3$, shows a static CDW instability.[31] Second, the pseudogap positions of $BaRuO_3$ systems are at about 0.1 eV, which is comparable with the CDW gap value of a static CDW system.[32] Third, the spectral weight change in Fig. 5(a) is quite similar to those predicted for the density wave materials.[33,34] We believe that the observation of the pseudogap in $4H$ $BaRuO_3$ provides further support for the CDW fluctuations as the origin of the pseudogap in the layered ruthenates.[35]

With such CDW fluctuations, there could be a partial gap opening in the k space on the Fermi surface, which could be closely related to the case of pseudogap formation in HTSC. Simultaneously, the suppression of the scattering channels on the Fermi surface could induce the reduction of $1/\tau$. Similar behaviors are observed in some density wave materials. $2H$-$TaSe_2$, which is a 2D CDW material, shows a weak gap structure, but retains its metallic characteristics across the CDW ordering transition temperature T_{CDW}. The absence of the increase of $\rho(T)$ at T_{CDW} was attributed to the partial-gap opening over a restricted region of the Fermi surface,[36] and furthermore, the reduction in $1/\tau$ is suggested to occur due to the collapse of a scattering channel with the formation of the CDW state.[37]

Although the metallic state of the $BaRuO_3$ systems is similar to the case of other static density wave systems, the ruthenates have quite distinct features. First, in both $4H$ and $9R$ $BaRuO_3$, no static density wave formation has been observed even down to very low T.[38] Second, the ruthenates do not show any strong anisotropy in their physical properties.[15] Third, the spectral weight transfer with the pseudogap formation is quite similar to that of the 1D-like CDW ordering. This strong 1D-like pseudogap feature is also distinguished from the 2D CDW materials such as $2H$-$TaSe_2$.[36] Fourth, the pseudogap positions show no significant T-dependent behavior, so it does not follow the BCS-like behavior for the density wave gap. Finally, a strong T-dependent suppression of $1/\tau$ occurs with a reduction in n with pseudogap formation. These distinct features, which could be related to the lack of the long-range ordering at any finite temperature, might be related to the quantum critical point fluctuation near a metal-insulator transition.[39] Further investigations to probe this possibility are highly desirable.

E. A systematic trend in the layered compounds, $BaMO_3$ (M=Ru or Ir)

In the layered compounds with the face sharing of the Ru(or Ir)O_6 octahedra, it was suggested that the strength of the quasi-1D-like metal bonding along the c axis could be a parameter which controls their physical properties.[3] The metal-bonding contribution in $9R$ $BaRuO_3$ becomes larger than that in $4H$ $BaRuO_3$, since the former has greater numbers of face sharings per single RuO_6 octahedron than the latter. The quasi-1D-like contribution will become even larger for $BaIrO_3$, since the $5d$ transition metal Ir ions could have a stronger metallic bonding character than the $4d$ transition metal Ru ions.[31]

It is quite interesting to see that there is a systematic trend in the $BaMO_3$ (M=Ru or Ir) compounds. From the optical spectra, we approximately estimated the pseudogap positions to be about 0.08 eV and 0.1 eV in $4H$ and $9R$ $BaRuO_3$, respectively. It was also reported that the optical gap position value of $BaIrO_3$ is about 0.15 eV.[31] As the quasi-1D-like

TABLE II. Summary of the physical properties in the layered materials [$BaMO_3$ (M=Ru and Ir)].

	$4H$ $BaRuO_3$	$9R$ $BaRuO_3$[a]	$BaIrO_3$[b]
Metal-bonding structure	two RuO_6	three RuO_6	three IrO_6
(Pseudo) Gap position	0.08 eV	0.1 eV	0.15 eV
Electric state at low T	Fermi-liquid-like	Crossover behavior from metallic to insulator-like states	Insulating

[a]Reference 3.
[b]Reference 31.

metal-bonding along c axis becomes stronger, the pseudogap (or gap) position in the ab plane seems to become higher. Moreover, the bonding strength seems to also be related to the transport properties. $4H$ $BaRuO_3$ has a metallic behavior even with a small reduction in n at a low T. $9R$ $BaRuO_3$ shows an interesting crossover from metallic to insulating-like states due to the significant reduction in n with decreasing T. $BaIrO_3$ seems to be an insulator (namely, $n=0$). A summary of these systematic changes is given in Table II. To confirm these interesting properties, it is useful to investigate further the physical properties of other $4d$ or $5d$ compounds with $4H$, $6H$, and $9R$ structures.

V. SUMMARY

$4H$ $BaRuO_3$ exhibits clear pseudogap formation in its optical spectra, similar to $9R$ $BaRuO_3$. From these observation, it can be concluded that $4H$ and $9R$ $BaRuO_3$ compounds can be another class of pseudogap systems in $4d$ electron systems. It looks like the strong suppression of the scattering rate, in spite of the carrier density, is responsible for their metallic states. Additionally, the subtle difference in electrodynamic parameters makes two $BaRuO_3$ systems have different temperature dependences of resistivity and magnetic susceptibility. It is expected that these materials will provide more insights on pseudogap phenomena in strongly correlated materials.

ACKNOWLEDGMENTS

We acknowledge H. Y. Choi and K. H. Kim for helpful discussion. We also thank the Inter-University Center for National Science Facilities at SNU and Pohang Accelerator Laboratory for allowing us to use some of their facilities. This work was supported by the Ministry of Science and Technology through the Creative Research Initiative program.

[1] Y. Maeno, H. Hashimoto, K. Yoshida, S. Nashizaki, T. Fujita, J.G. Bednorz, and F. Lichtenberg, Nature (London) **372**, 532 (1994).
[2] P. Kostic, Y. Okada, N.C. Collins, Z. Schlesinger, J.W. Reiner, L. Klein, A. Kapitulnik, T.H. Geballe, and M.R. Beasley, Phys. Rev. Lett. **81**, 2498 (1998).
[3] Y. S. Lee, J. S. Lee, K. W. Kim, T. W. Noh, Jaejun Yu, E. J. Choi, G. Cao, and J. E. Crow, Europhys. Lett. **55**, 280 (2001).
[4] H. Ding, T. Yokoya, J.C. Campuzano, T. Takahashi, M. Randeria, M.R. Norman, T. Mochiku, K. Kadowaki, and J. Giapintzakis, Nature (London) **382**, 51 (1996).
[5] M.R. Norman, H. Ding, M. Randeria, J.C. Campuzano, T. Yokoya, T. Takeuchi, T. Takahashi, T. Mochiku, K. Kadowaki, P. Guptasarma, and D.G. Hinks, Nature (London) **392**, 157 (1998).
[6] Ch. Renner, B. Revaz, J.-Y. Genoud, K. Kadowaki, and Ø. Fischer, Phys. Rev. Lett. **80**, 149 (1998).
[7] S. Donovan, A. Schwartz, and G. Grüner, Phys. Rev. Lett. **79**, 1401 (1997).
[8] M. Dressel, B. Gorshunov, N. Kasper, B. Nebendahl, M. Huth, and H. Adrian, J. Phys.: Condens. Matter **12**, 1633 (2000).
[9] L. Degiorgi, Rev. Mod. Phys. **71**, 687 (1999).
[10] P.C. Donohue, L. Katz, and R. Ward, Inorg. Chem. **4**, 306 (1965).
[11] J.M. Longo and J.A. Kafalas, MRS Bull. **3**, 687 (1968).
[12] S.T. Hong and A.W. Sleight, J. Solid State Chem. **128**, 251 (1997).
[13] M.K. Lee, C.B. Eom, W. Tian, X.Q. Pan, M.C. Smoak, F. Tsui, and J.J. Krajewski, Appl. Phys. Lett. **77**, 364 (2000).
[14] M.K. Lee, C.B. Eom, J. Lettieri, I.W. Scrymgeour, D.G. Schlom, W. Tian, X.Q. Pan, P.A. Ryan, and F. Tsui, Appl. Phys. Lett. **78**, 329 (2000).
[15] J.T. Rijsssenbeek, R. Jin, Yu. Zadorozhny, Y. Liu, B. Batlogg, and R.J. Cava, Phys. Rev. B **59**, 4561 (1999).
[16] F. Wooten, *Optical Properties of Solids* (Academic, New York, 1972).
[17] J.S. Ahn, J. Bak, H.S. Choi, T.W. Noh, J.E. Han, Yunkyu Bang, J.H. Cho, and Q.X. Jia, Phys. Rev. Lett. **82**, 5321 (1999).
[18] H.S. Choi, Y.S. Lee, T.W. Noh, E.J. Choi, Y. Bang, and Y.J. Kim, Phys. Rev. B **60**, 4646 (1999).
[19] J.W. Allen and J.C. Mikkelsen, Phys. Rev. B **15**, 2952 (1977).
[20] T. Timusk and D. Tanner, in *Physical Properties of High Temperature Superconductors II*, edited by D. M. Ginsberg (World Scientific, Singapore, 1992), Chap. 5.
[21] In this analysis, the values of m^* are estimated to be too large. This is because $\chi(T)$ in $4H$ $BaRuO_3$ might be largely enhanced due to the ferromagnetic fluctuation.
[22] In this temperature region, the very weak T dependences of $n(T)$ and $m^*(T)$ are observed. So, the T^2 dependence is expected to come from electron-electron scatterings.
[23] K. Miyake, T. Matsuura, and C.M. Varma, Solid State Commun. **71**, 1149 (1989).

[24] N. W. Ashcroft and N. D. Mermin, *Solid State Physics* (Saunders College Publishing, Philadelphia, 1976).
[25] I.I. Mazin and David J. Singh, Phys. Rev. Lett. **79**, 733 (1997).
[26] If the enhancement of $\chi(T)$ in $4H$ $BaRuO_3$ is due to the ferromagnetic fluctuations, its contribution will provide different values of n and m^*, especially m^*.
[27] D.N. Basov, R. Liang, B. Dabrowski, D.A. Bonn, W.N. Hardy, and T. Timusk, Phys. Rev. Lett. **77**, 4090 (1996).
[28] C.C. Homes, T. Timusk, R. Liang, D.A. Bonn, and W.N. Hardy, Phys. Rev. Lett. **71**, 1645 (1993).
[29] T. Timusk and B. Statt, Rep. Prog. Phys. **62**, 61 (1999).
[30] G.R. Stewart, Rev. Mod. Phys. **56**, 755 (1984).
[31] G. Cao, J.E. Crow, R.P. Guertin, P.F. Henning, C.C. Homes, M. Strongin, D.N. Basov, and E. Lochner, Solid State Commun. **113**, 657 (2000).
[32] G. Grüner, *Density Waves in Solids* (Addison-Wesley, Reading, MA, 1994).
[33] L. Degiorgi, M. Dressel, A. Schwartz, B. Alavi, and G. Grüner, Phys. Rev. Lett. **76**, 3838 (1996).
[34] M. Tinkham, *Introduction to Superconductivity* (McGraw-Hill, New York, 1975).
[35] Up to now, the pseudogap onset temperature T^* in $4H$ $BaRuO_3$ is not clear. In contrast to other pseudogap systems, the signature of the pseudogap is not clearly observed in $\rho(T)$ and $\chi(T)$. This could be related to its nonmagnetism and a fluctuation type of instability. In $\sigma_1(\omega)$, a weak gaplike feature is observed even at 300 K. So, T^* is expected to position above 300 K, which has been observed in other CDW materials, such as $K_{0.3}MoO_3$ and $2H$-$TaSe_2$.
[36] V. Vescoli, L. Degiorgi, H. Berger, and L. Forró, Phys. Rev. Lett. **81**, 453 (1998).
[37] T. Valla, A.V. Fedorov, P.D. Johnson, J. Xue, K.E. Smith, and F.J. DiSalvo, Phys. Rev. Lett. **85**, 4759 (2000).
[38] While it is possible that a relatively long time scale of the CDW fluctuations could result in the removal of degeneracy of the lattice modes, the splitting of IR-active phonons in our spectra was not detected within our experimental resolution. On the other hand, a recent Raman study shows the phonon splitting of the E_{2g} mode of the face-shared oxygen with decreasing T [E. J. Oh *et al.* (unpublished)].
[39] S. Sachdev, *Quantum Phase Transitions* (Cambridge University Press, Cambridge, England, 2000).